Residual Stiffness Assessment of Failed RC Beam Structure by FE Model Updating

J. M. W. Brownjohn[1] and P. Q. Xia[2]

Abstract

For a reinforced concrete (RC) beam structure subject to a mid-span point load, failure in tension is deemed to occur when steel reinforcement on the tension side has yielded. When unloaded from this post-serviceability cracking stage, the residual stiffness of the failed structure is difficult to estimate. This paper presents a new method for the residual stiffness assessment of a failed RC member such as a beam or one way narrow slab at the post-serviceability cracking stage based on dynamic testing and finite element (FE) model updating. The failed zones are simulated using damaged beam elements in an FE model of the structure and the measured modal properties i.e. frequencies and mode shapes are used as the reference data for model updating. Through a procedure of sensitivity-based updating, the stiffness distribution along the member can be obtained, leading to identification of location and extent of the damaged (failed) region.

Key words: stiffness assessment, reinforced concrete, beam structure, post-serviceability, finite element model updating

---

[1]Associate Professor, [2]Ph.D Student
School of Civil and Structural Engineering
Nanyang Technological University
Nanyang Avenue
Singapore 639798

Nomenclature

A	area of cross-section
$A_q(i\omega)$	Fourier transform of acceleration response $a_q(t)$
c_b	depth of neutral axis of reinforced concrete beam
D_i	damage index
E	Young's modulus
EI	stiffness
f	frequency in Hz
$F_p(i\omega)$	Fourier transform of force input $f_p(t)$
$H_{pq}(i\omega)$	frequency response function (FRF) between position p and q
i	complex number
I	moment of inertia of cross-section
MAC	modal assurance criterion
n	Young's modulus ratio of steel and concrete
p	position of force
q	position of acceleration measurement
Δ_f	frequency difference between updated and measured
ε	strain
ϕ	mode shape vector
σ	stress
ω	circular natural frequency

Superscript

f	failed
T	transpose of vector
u	updated
*	conjugation of complex number
′	quantity of top steels in beam

Subscript

c	concrete
s	steel and slab
b	beam
a	analysis
e	experiment
t	transformed quantity
cr	cracked
m	midspan and measured
u	updated

1. Introduction

The deflection, as a measure of stiffness, of a reinforced concrete (RC) member determines an operating range for serviceability and post-serviceability before rupture. The load-deflection relationship of a RC beam, shown in Fig. 1 (Nawy, 1990), is essentially composed of three regions prior to rupture:

(1) a very limited or even non-existent pre-cracking stage where a structural member is crack-free;

(2) post-cracking stage where the structural member develops acceptable controlled cracking both in distribution and width (most beams lie in this region at service loads); and

(3) post-serviceability cracking stage where the stress in tension reinforcement reaches the limit state of yielding, the beam is considered at this stage to have structurally failed by initial yielding of tension steel.

Methods for estimating the stiffness of a RC beam and one way slab at the stage I and II are available (Nawy, 1990) and can give adequate basic background on the effect of cracking on the stiffness of the member. At the stage III or post-serviceability cracking stage, it is difficult to estimate the residual stiffness due to the yielding of the tension steel in the RC beam (assuming it to be an under-reinforced member). However, it is important to recognize the reserve deflection capacity as a measure of ductility in structures in earthquake zones and in other applications where the probability of overload is high.

Recently, the finite element (FE) model updating method (Mottershead and Friswell, 1993) for damage identification (Doebling, et. al 1998) based on dynamically measured data such as measured frequencies and mode shapes has received some attention. This method combines experimental modal analysis and finite element analysis, rather than purely relying on numerical analysis and is designed for correcting the uncertainties in modeling, geometry, material and analysis to improve the analytical estimates of performance by systematic comparison with experimental results. In two

different applications (Brownjohn and Xia, 1999, 2000) the method was used to identify damage in a model bridge and to characterize the structural properties of a prototype bridge. In the present application, because the method can correct any parametric uncertainty in a model, it provides a possibility to accurately assess the residual stiffness of the RC structures at post-serviceability cracking stage.

This investigation described in this paper focused on the application of the method to residual stiffness assessment of a simulated pedestrian RC beam bridge model which was loaded to the post-serviceability cracking stage. The testing was conducted during a student practical exercise to study the serviceability and ultimate performance of the beam structures. Extensively instrumented beam structures were studied at various stages of mid-span loading through serviceability load (to achieve a specified deflection), load for failure (yield of tension steel) and rupture. Vibration testing was done on one simply supported 5*m* span beam bridge model in the original unloaded state so that a reliable FE model could be set up based on the measured data. After failure but before rupture the structure was retested to provide reference data to estimate the residual stiffness of the failed structure. Based on the stiffness distribution along the beam span identified by FE model updating, the location and extent of damage in the RC beam were determined.

2. Stiffness Estimation at Cracking Stage I and II

The detailed geometry of investigated RC bridge structure is shown in Fig. 2. It comprised a shallow lightly reinforced slab component with two deep reinforced edge beams. The edge beams were nominally 250*mm* deep by 150*mm* wide. The bridge deck

had overall 1*m* width and 5*m* length and was simply supported at the ends on two concrete blocks as shown in Fig. 2.

At the first stage in region I shown in Fig. 1, the flexural stiffness of the bridge deck *EI* can be estimated using Young's modulus of concrete E_c multiplied by the moment of inertia of the uncracked RC cross section which is transformed to the same material. The value of E_c for normal-weight concrete can be estimated using the ACI empirical expression (Nawy, 1990), $E_c = 4730\sqrt{\sigma_c}$ (N/mm^2) where σ_c is compressive strength of concrete measured at 28 days after casting. Based on sample cube tests, $E_c = 2.99\times10^4 (N/mm^2)$. The area of steel reinforcement A_s is replaced by an equivalent concrete area $(E_s / E_c)A_s$ in which E_s is the modulus of the reinforcing steel. The transformed moment of inertia of one edge beam I_{bt} and of slab component I_{st} with rectangular cross-section shown in Fig. 2 and their center of gravity of the transformed section $\bar{y}_{bt}$ and $\bar{y}_{st}$ are given as follows,

$$I_{bt} = \tfrac{1}{12}bh^3 + bh(\bar{y}_{bt} - \tfrac{1}{2}h)^2 + (n-1)A_s(d-\bar{y}_{bt})^2 + (n-1)A_s^{'}(\bar{y}_{bt} - d^{'})^2 \quad (1)$$

$$\bar{y}_{bt} = \frac{\tfrac{1}{2}bh^2 + (n-1)A_s d + (n-1)A_s^{'}d^{'}}{bh + (n-1)A_s + (n-1)A_s^{'}} \quad (2)$$

$$I_{st} = \tfrac{1}{12}b_1h_1^3 + b_1h_1(\bar{y}_{st} - \tfrac{1}{2}h_1)^2 + (n-1)A_{s1}(d_1 - \bar{y}_{st})^2 \quad (3)$$

$$\bar{y}_{st} = \frac{\tfrac{1}{2}b_1h_1^{\,2} + (n-1)A_{s1}d_1}{b_1h_1 + (n-1)A_{s1}} \quad (4)$$

where, $n = E_s / E_c$ is the modulus ratio. A_s and $A_s^{'}$ are the areas of top and bottom steels in one edge beam respectively. A_{s1} is the total areas of steels in the slab. The values of dimensions and areas are given in Fig. 2. After substitution of relevant values into

equations (1), (2), (3) and (4), the transformed moments of inertia were calculated as $I_{bt} = 2.68 \times 10^8 mm^4$, $I_{st} = 1.71 \times 10^8 mm^4$ and the overall transformed moment of inertia of the deck $I_t = 2I_{bt} + I_{st} = 7.07 \times 10^8 mm^4$.

At the second stage of load-deflection relationship (region II shown in Fig. 1), the edge beams underwent varying degrees of cracking along the span, corresponding to the stress and deflection levels at each section. Hence cracks were wider and deeper at midspan. When flexural cracking developed, the flexural rigidity of the section was reduced as the contribution of the concrete along the beams in the tension zone reduced substantially and the depth of the compression zone reduced. As the cracked zone expanded, stiffness continued to decrease, reaching a lower-bound value corresponding to the reduced moment of inertia of the completely cracked section. At this state the contribution of tension-zone concrete to the stiffness was neglected. The strain and stress distributions through the depth of the cracked rectangular concrete beam section at this stage are shown in Fig.3. Based on extensive testing verification (Spiegel and Limbrunner, 1998), the following assumptions were made:

(1) the strain distribution across the depth of a typical cracked concrete section is assumed to be linear;

(2) concrete does not resist any tension; and

(3) both concrete and steel are within the elastic limit.

In terms of the assumptions and the horizontal force equilibrium in cross section, the moment of inertia of the cracked beam section I_{bcr} can be determined as follows,

$$I_{bcr} = \tfrac{1}{3} b c_b^3 + n A_s (d - c_b)^2 + (n-1) A_s^{'} (c_b - d^{'})^2 \qquad (5)$$

where the value of neutral axis depth c_b can be obtained from

$$\tfrac{1}{2} bc_b^2 + [A_s n + (n-1)A_s^{'}]c_b - nA_s d - (n-1)A_s^{'} d^{'} = 0 \quad (6)$$

In equation (5), the first term denotes the moment of inertia of the compressive area bc_b about the neutral axis, namely, the base of the compression rectangle, neglecting the section area in tension below the neutral axis. The reinforcing area was scaled by *n* to transform to an equivalent concrete area for contribution to the section stiffness. The moment of inertia of the steel about its own axis was disregarded as negligible.

From equations (5) and (6), the moment of inertia for one edge beam was calculated as $I_{bcr} = 5.28 \times 10^7 mm^4$, then the overall moment of inertia of the cracked cross section of the deck was given as $I_{cr} = 2I_{bcr} + I_{st} = 2.77 \times 10^8 mm^4$ which was approximately $0.2I_{bt}$ and $0.39I_t$ respectively. Of course only part of the beam cross section was cracked and (from Fig. 3a) the uncracked area below the neutral axis along the beam span contributed to the overall beam rigidity. The actual overall stiffness of the cracked bridge deck lies between $E_c I_t$ and $E_c I_{cr}$, approaching $E_c I_{cr}$ as steel approaches yield point. When the beam enters the post-serviceability stage, the overall stiffness value drops below $E_c I_{cr}$.

3. Static and Dynamic Testing

In the static load testing, midspan loads were applied in increments of 2~5kN by a hydraulic jack as shown in Fig. 7 until the maximum load of 47.3 kN was sustained, (compared to the design value of 40 kN). Beam deflections obtained by LVDTs and steel reinforcement strains from electrical resistance strain gauges were recorded. Fig. 4 shows

the measured load-deflection relationship showing regions I, II and III. The cracking developed at midspan is shown highlighted by marker pen in Fig. 5.

Vibration testing on the bridge model was conducted first before any loading and then after failure. Techniques of modal analysis (Ewins, 1984) were used to identify the dynamic properties such as frequencies, mode shapes and damping ratios of a structure through input (excitation) and output (response) signals using the test set up shown in Fig. 6. There were 22 measurement points totally and one excitation point which was kept in the same location on the bridge deck surface during the testing. Excitation by both instrumented hammer (5.5kg) and electrodynamic long stroke inertial shaker were used to guarantee the quality of test data. Both techniques apply a broadband excitation, the shaker via a continuous chirp or fast sine swept signal (Godfrey, 1993) and the hammer by impulsive load (Fig. 7). Response signals obtained from ICP accelerometers stuck at the measurement points were recorded through analog to digital converter via a sixteen channel data acquisition, control and analysis system also used to generate the shaker excitation control signal. Data acquired in time domain were used to determine the frequency response function (FRF) $H_{pq}(i\omega)$ as follows,

$$H_{pq}(i\omega) = \frac{A_q(i\omega)A_q^*(i\omega)}{F_p(i\omega)A_q^*(i\omega)} \tag{7}$$

An example acceleration response time history from an accelerometer at a measurement point by shaker excitation and an FRF curve are shown in Fig. 8 and Fig.9 respectively. From the FRFs, the measured frequencies and corresponding mode shapes of the structure were obtained by using modal analysis technique (Ewins, 1984). The measured frequencies f_m are listed in the second column in Table 1. The measured mode

shapes are shown in the first column in Fig. 10 which shows obvious responses at the elastic supports (concrete blocks).

The failed bridge deck was tested again using the same method as for preload testing. The measured frequencies f_m are listed in the sixth column in Table 1. The measured mode shapes are shown in the second column in Fig. 10. After compared the measured data, it can be seen that the frequencies of the damaged bridge structure were slightly reduced and the slightly sharper curvature of the first and third mode shapes at midspan of the failed structure, comparing with its undamaged structure, was produced due to the large stiffness reduction in the failure zone. The measured frequencies and mode shapes were used as reference data for FE model updating of the damaged structures.

4. Stiffness Assessment at Cracking Stage III

It is difficult to estimate the residual stiffness of RC beam structure at the post-serviceability cracking stage III due to the yielding of the tension steel in the RC beam as described previously. However, it is possible to estimate the stiffness by using the FE model updating method due to its ability to identify uncertainties in the structure. The detailed procedure of the sensitivity analysis based FE model updating can be seen in the reference (Brownjohn and Xia, 2000).

'Damaged' FE model

Model updating necessitates an appropriate FE model of the structure. In the preparation of FE model for updating, it is important that modeling uncertainties can be assessed quantitatively as far as possible. For a damaged structure, the damaged zones

will not be generally contained in a FE model unless some special considerations are incorporated. In this case, a kind of 'damaged' or 'weakened' beam model (Brownjohn and Xia, 1999) was used to simulate the cracked zone at midspan of the edge beam components. A 'damaged' beam model is shown in Fig. 11. The physical and geometrical parameters of the 'damaged' element depend on the damage extent.

To represent the large responses at the supports of the structure (Fig. 10), the boundary conditions were taken as elastic supports in the form of eight linear springs in the FE model. Two side edge beam components were modeled using 3D beam elements and four 'weak' beam elements were located around midspan. The top slab component of the deck was modeled using shell elements. The resulting FE model is shown in Fig. 12. It should be pointed out that if the parameters of 'weak' beam elements take the real values for the damage zones, then the FE model is taken to represent the damaged structure, but if the parameters match those for the rest of the beam the FE model represents the undamaged structure.

Model Updating of Undamaged Structure

In order to accurately estimate residual stiffness of the failed RC bridge structure, it is fatal to have a reliable FE model with correct parameters and boundary conditions which necessitates model updating for the undamaged structure. Generally, a model updating procedure includes three aspects (Brownjohn and Xia, 1999, 2000):

(1) selection of responses such as measured frequencies and mode shapes as reference data for updating;

(2) selection of uncertain physical and geometrical parameters to which changes in the selected responses must be sensitive; and

(3) model tuning which is an iterative process to estimate the selected parameters based on the reference data.

In this exercise, stiffness of springs at the boundary supports, Young's modulus of concrete E_c, mass density of concrete and moment of inertia of the edge beam I_{bt}, were selected as uncertain parameters to update. The model tuning is a semi-automatic process using the FEMtools software (*FEMtools*, 1998). During the updating, it is necessary to make some manual adjustments e.g. support spring stiffness to provide a starting point. Without a reasonable starting point, the iterative updating procedure may not converge to a solution (Brownjohn and Xia, 1999, 2000).

After model updating based on the measured frequencies and mode shapes for the undamaged structure, the updated value of Young's modulus of concrete was equal to $E_c^u = 2.79 \times 10^4 N/mm^2$, a reduction by 6.69% compared to its original estimate. The updated value of moment of inertia of the edge beam was $I_b^u = 3.23 \times 10^8 mm^4$ compared to original estimate $I_{bt} = 2.68 \times 10^8 mm^4$.

The success of model updating can be judged by correlation indicators such frequency difference Δ_f between FE model and measurement and by the modal assurance criterion or *MAC* (Allemang and Brown, 1982) defined by,

$$MAC(\phi_a, \phi_e) = \frac{\left|\phi_a^T \phi_e\right|^2}{(\phi_a^T \phi_a)(\phi_e^T \phi_e)} \tag{8}$$

Given a set of experimental modes and a set of predicted modes, a matrix of *MAC* values can be computed. The matrix could indicate clearly which experimental mode relates to which predicted mode. The mode shapes with a *MAC* value equal to 100% represent a

perfect correlation, modes which are completely orthogonal have 0% *MAC*. Generally, it is found that a value in excess of 90% should be attained for correlated modes.

The updated frequencies f_u and the differences Δ_f are listed in the first and third column in Table 1, respectively. The *MAC* values are listed in the fourth column in Table 1. The low Δ_f and high *MAC* values show an excellent correspondence between updated FE model and test model. The visualization of mode shapes shown in the first column in Fig. 13 also indicated the correspondence between the updated FE model and measured model. These correspondences gave a confidence that the updated model can be taken as a reliable initial FE model for updating the failed structure so as to obtain an accurate estimation of the residual stiffness.

Stiffness Assessment of Failed Structure

After loading to the ultimate limit state, the cracks were wider and deeper at midspan, whereas narrower and shallower minor cracks developed towards the supports. The varying cracks along the beam span produced a varying reduction of the moment of inertia resulted in a varying reduction of the stiffness along the beam. Hence the moment of inertia of the beam was selected as uncertain parameter to update in the damaged FE model. The distribution of the moment of inertia along the beam span after updating determined the stiffness distribution of the beam. The starting value of the moment of inertia of the beam element was taken as the value of I_b^u except for the 'weak' beam at the midspan. The wide and deep cracks at the mispan should lead to serious reduction of moment of inertia at midspan whose starting value was taken as I_{bcr} which was the estimated value of moment of inertia at the midspan at the post-cracking stage II and would become the value at the midspan at the post-serviceability stage III after updating

based on the measured data from the failed RC structure. The length of a 'weak' beam at midspan was taken as $0.12m$. The length of two 'weak' beams was approximately equal to the length of the damaged zone at midspan. Besides the moment of inertia, Young's modulus was also selected as an updating parameter at the midspan. The starting value of Young's modulus was taken as E_c^u.

After the tuning procedure, the updated frequencies f_u and the differences Δ_f are listed in the fifth and seventh column in Table 1, respectively. The *MAC* values are listed in the eighth column in Table 1. The Δ_f values were very small and the *MAC* values were very high. The pairing of mode shapes of the failed structure with those from the updated 'damaged' FE model is shown in the second column in Fig. 13 in which the consistency of the updated model with the measured model can be seen.

At midspan, the updated value of Young's modulus and moment of inertia were $E_{bm}^f = 2.15\times10^3 N/mm^2$ and $I_{bm}^f = 3.14\times10^7 mm^4$ respectively (all values of moment of inertia at midspan beam are listed in Table 2 for convenient look). Thus, The residual stiffness of the failed bridge deck at midspan at the post-serviceability cracking stage III was estimated as $2E_{bm}^f I_{bm}^f + E_c^u I_{pt} = 4.91\times10^{12} Nmm^2$, smaller than the estimated value $E_c^u I_{cr} = 7.72\times10^{12} Nmm^2$ at the post-cracking stage II. According to the updated values of moment of inertia along the beam, the distribution of stiffness *EI* along the failed deck at the post-serviceability cracking stage III can be obtained and is shown in Fig. 14. It is obvious that the smallest stiffness was at midspan of the failed deck and the stiffness increased gradually towards the supports.

It should be pointed out that the moment of inertia of RC beam depends on the square of depth of neutral axis through equation (5), so the distribution of stiffness along a beam will be similar to the distribution of depth of neutral axis along the beam. Fig. 15 shows the measured distribution of depth of neutral axis of the beam under the ultimate limit state during the static testing. The neutral axis depth for the beam was obtained by linear interpolation of strain values from the top and bottom steels in the edge beam and is defined as c_b in Fig. 3. The negative neutral axis depth at the midspan means that the up and down steels in the edge beam were all in tension at the ultimate limit state. Values above the beam are possible due to the contribution of the slab element with uneven surface. The distributions in Fig. 14 and Fig. 15 are remarkably similar.

In terms of the stiffness distribution of the failed deck, the location and extent of damage along the deck also can be obtained. The cross-section with reduction of stiffness located the damage along the deck. A damage index D_i which can determine the extent of damage is defined as,

$$D_i = \frac{\Delta(EI)}{(EI)_o} \times 100\% \tag{9}$$

where $\Delta(EI)$ denotes the change in stiffness between undamaged and damaged cross-section of the deck and $(EI)_o$ denotes the original stiffness of the undamaged cross section of the deck. Fig. 16 shows the damage index D_i along the deck. Obviously, the extent of damage at midspan of the failed deck was most serious, at 71.4%.

5. Discussion

In order to be successful in model updating, some manual tuning of values for selected parameters is necessary prior to tuning procedure, especially in the case of a large difference between initial estimates and true values of selected parameters. This occurs when parameters are significantly changed by serious damage or structural failure, or when there is no reasonable estimate available, such as for boundary condition stiffness. The manual tuning to date has been done based on experience but there are some systematic procedures available.

Meanwhile, for a simple RC structure like this bridge deck, it would also normally be necessary to analyze the structure at the pre-cracking stage I and post-cracking stage II. These analyses can supply reliable initial information for successful model updating of the failed structure at the post-serviceability cracking stage III for correct damage assessment. If the model updating goes straight to the damaged case, it is unlikely to be successful due to numerous and large uncertainties in the FE model. For example, in this exercise, boundary condition parameters obtained from stage I measurements and estimated midspan beam inertia at the stage II were taken as the reasonable initial value for the failed deck updating. Without doing this, the updating cannot converge to a solution for accurate estimation of parameters. It may be possible to go straight to model updating for the damaged case when the original structural conditions are well known, i.e. there is a ‘baseline’ model, but this is not the normal case.

The investigation described in this paper was a laboratory exercise which can be extended to be applicable to real bridges e.g. highway bridges. Such kind of bridges may be tested for dynamic properties by using hammer excitation and is not necessary to close

the bridge during the measurement. It is suggested that the existing bridges should be conducted the dynamic testing for establishment of bridge management data (Hearn, 1998) which can be used for structural condition assessment (Aktan et al, 1996) in case the bridge is damaged accidentally.

Conclusions

The model updating method based on the dynamic measurements can identify the residual stiffness of the failed reinforced concrete beam structure that is at the post-serviceability cracking stage III. The identified stiffness distribution along the beam can locate the damage in the structure and determine the extent of the damage.

Using a “damaged” beam element to simulate the damaged area in the structure is a practical and convenient way to model the failed structure in FE analysis. The estimated values of geometrical parameters of the beam at the post-cracking stage II can be taken as the initial values of the “damaged” beam elements for failed model updating.

References

Aktan, A. E., Farhey, D. F., Brown, D. L., Dalal, V., Helmicki, A. J., Hunt, V. J., and Shelley, S. J. (1996). "Condition assessment for bridge management." Journal of Infrastructure Systems, ASCE, 2(3), 108-117.

Allemang, R. J., and Brown, D. L. (1982). "A correlation coefficient for modal vector analysis." *Proceedings of the 1st International Modal Analysis Conference*, SEM, Orlando, Florida, Vol. I, 110-116.

Brownjohn, J. M. W., and Xia P. Q. (1999). "Finite element model updating of a damaged structure." *Proceedings of the 17th International Modal Analysis Conference*, SEM, Kissimmee, Florida, Vol. I, 457-462.

Brownjohn, J. M. W., and Xia P. Q. (2000). "Dynamic assessment of curved cable-stayed bridge by model updating." *Journal of Structural Engineering*, ASCE, 126(2), 252-260.

FEMtools User Manual (1998), Version 1.4, Dynamic Design Solutions, Belgium.

Doebling, S. W., Farrar, C. R., and Prime, M. B. (1998). "A summary review of vibration-based damage identification methods." *The Shock and Vibration Digest*, 30(2), 9-105.

Ewins, D.J. (1984). *Modal Testing: Theory and Practice*, Research Studies Press LTD. John Wiley.

Godfrey, K. (1993). *Perturbation Signals for System Identification*, Prentice-Hall Inc.

Hearn, G. (1998). "Condition data and bridge management system." *Structural Engineering International*, IABSE, 8(3), 221-225.

Mottershead, J. E., and Friswell, M. I. (1993). "Model updating in structural dynamics: a survey," *Journal of Sound and Vibration*, Academic Press, 167(2), 347-375.

Nawy, E. G. (1990). *Reinforced Concrete*, 2nd Edition, Prentice-Hall, Inc.

Spiegel, L., and Limbrunner, G. F. (1998). *Reinforced Concrete Design*, 4th Edition, Prentice-Hall Inc.

Table 1 Correlation between FE Updating and Measurement

Undamaged Structure				Damaged Structure			
f_u (Hz) (1)	f_m (Hz) (2)	Δ_f (%) (3)	MAC (%) (4)	f_u (Hz) (5)	f_m (Hz) (6)	Δ_f (%) (7)	MAC (%) (8)
13.3	12.9	3.20	98.8	10.0	10.0	-0.40	99.7
31.3	33.0	-5.12	97.6	32.0	32.2	-0.76	99.0
44.5	42.6	4.40	97.3	41.1	40.8	0.69	97.7
74.1	70.6	4.99	96.6	70.2	68.8	1.98	93.2
78.2	81.4	-3.95	98.2	78.6	78.5	0.13	97.6

$\Delta_f = (f_u - f_m)/f_m \times 100\%$

Table 2 Moment of Inertia of Cross-section at Midspan Beam

Symbol	Value (mm^4)	Physical Meaning
I_{bt}	2.68×10^8	Transformed value at pre-cracking stage I
I_b^u	3.23×10^8	Updated ('true')value at pre-cracking stage I
I_{bcr}	5.28×10^7	Estimated value at post-cracking stage II
I_{bm}^f	3.14×10^7	Updated ('true') value at post-serviceability stage III

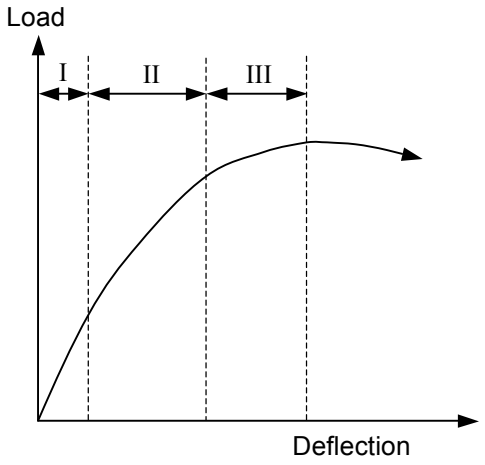

Fig. 1 Load-Deflection Relationship of Beam
Region I, Pre-cracking Stage;
Region II, Post-cracking Stage;
Region III, Post-serviceability Stage

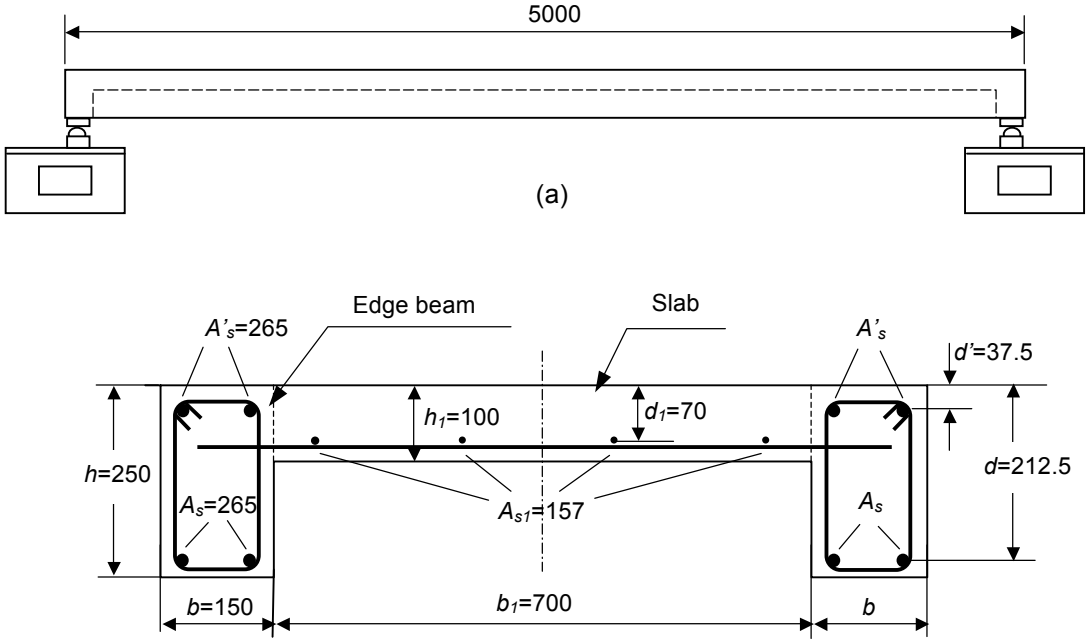

Fig. 2 Schematic of Reinforced Concrete Bridge Deck
(a) Span Unit with Simple Supports;
(b) Cross-section, Unit: Length(*mm*), Area(mm^2)

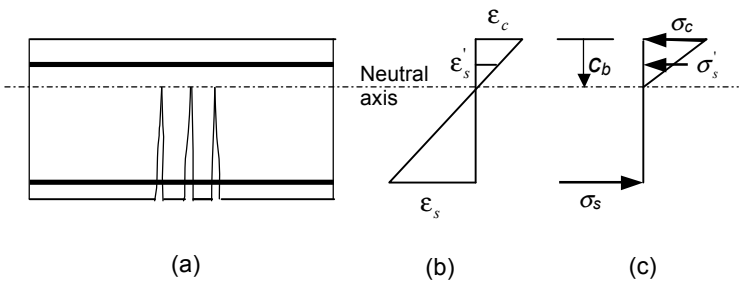

Fig. 3 Stress and Strain Distribution of Cracked Reinforced Concrete Beam: (a) Geometry; (b) Strain; (c) Stress

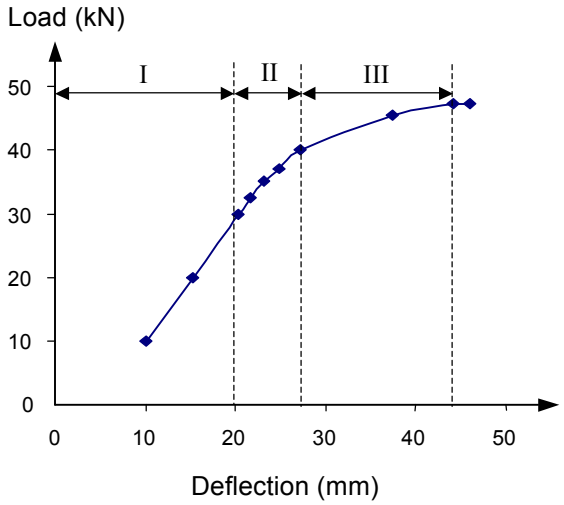

Fig. 4 Measured Load-Deflection Relationship of Deck

Fig. 5 Cracks at Midspan of Beam

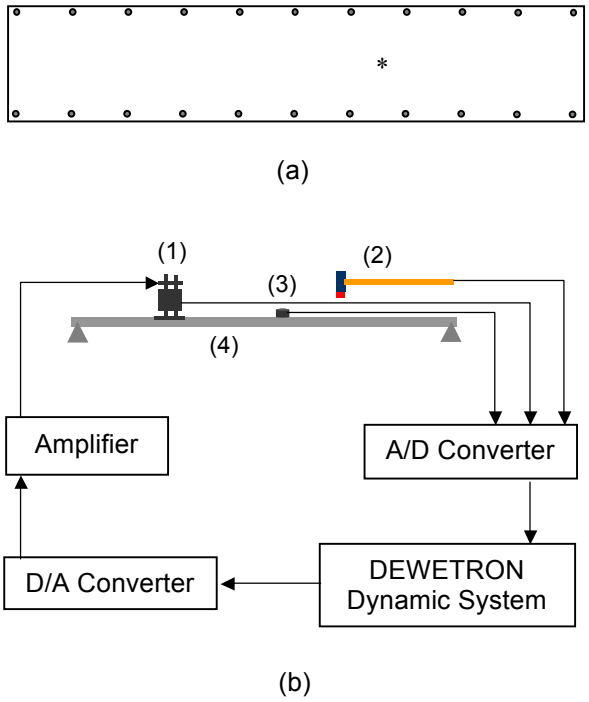

Fig.6 Vibration Testing Set-up for RC Bridge Deck
(a) Measurement Points ◦ and Excitation Point ∗
(b) Diagram: (1) Shaker; (2) Hammer;
(3) Accelerometer; (4) Deck

Fig. 7 Vibration Testing Using Instrumented Hammer and Experimental Set-up

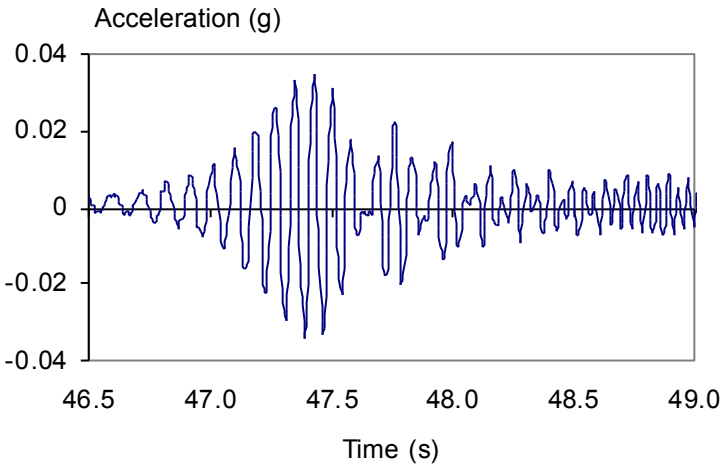

Fig. 8 Time History of Acceleration Response due to Chirp Excitation

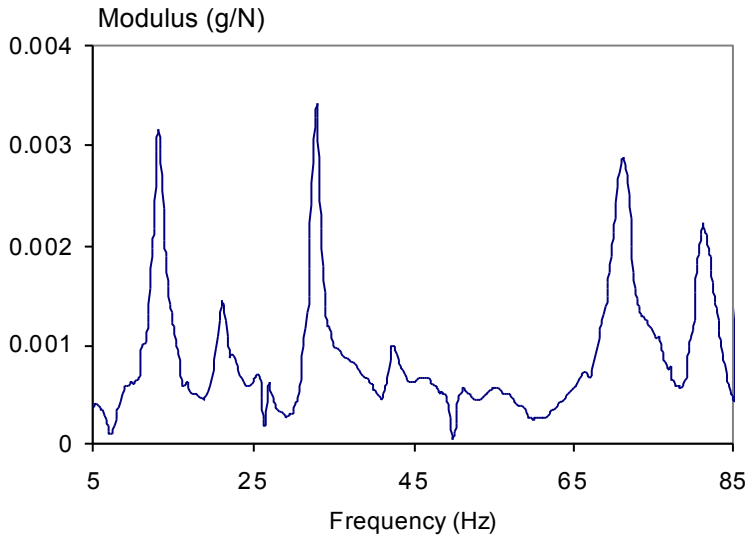

Fig.9 Measured FRF Magnitude at One Point

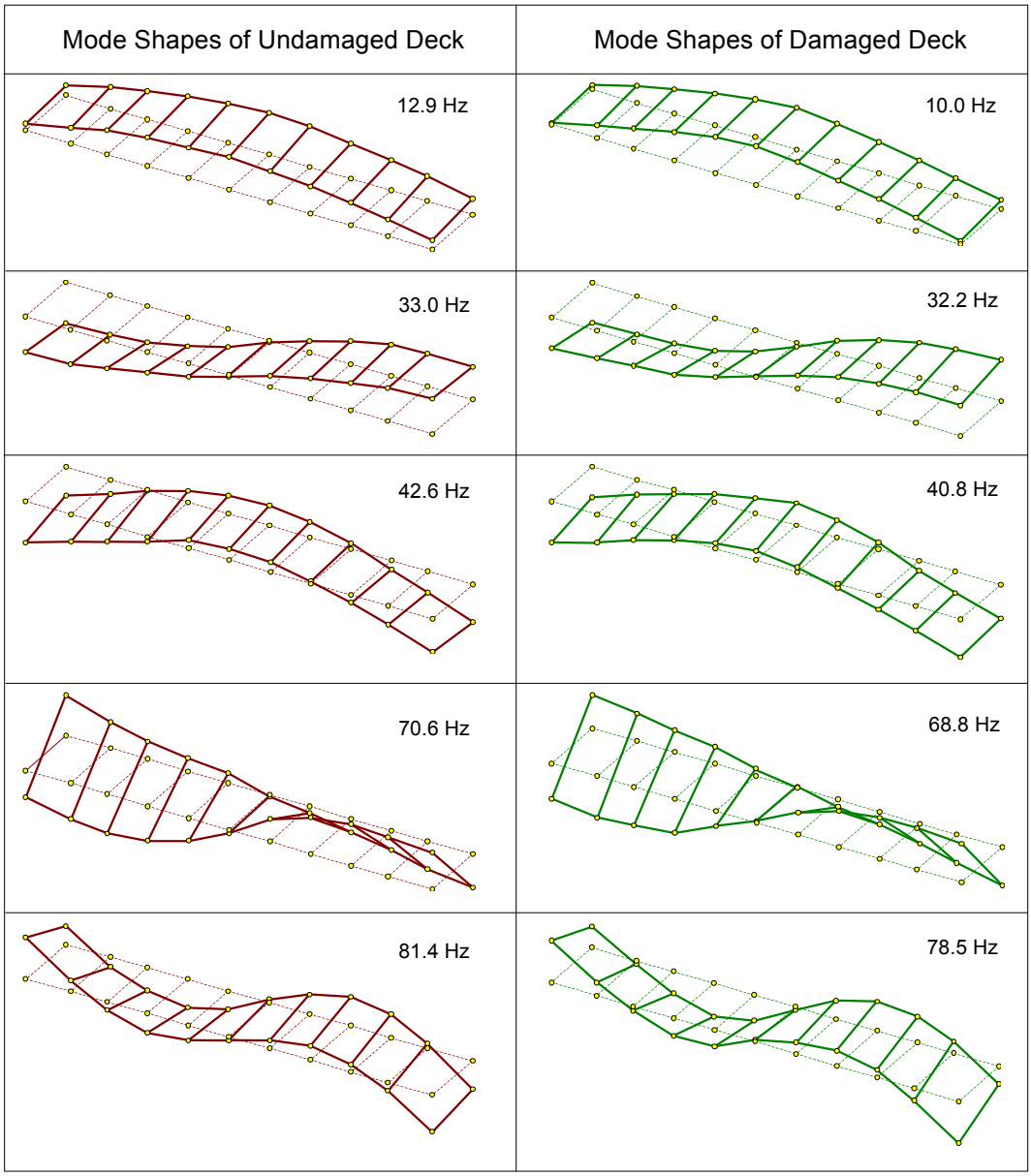

Fig.10 Measured Frequencies and Mode Shape of Deck
····· Undeformed; —— Deformed; ∘ Test Point

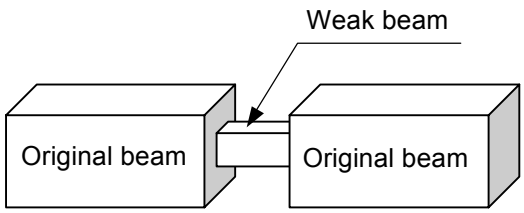

Fig. 11 A ‘Damaged” Beam Model

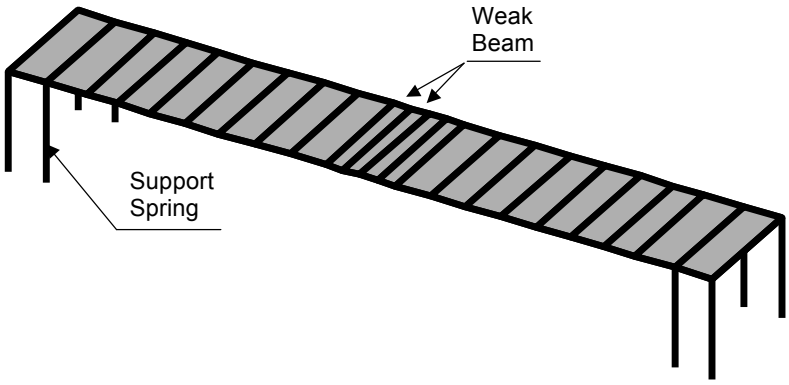

Fig. 12 FE Model of Bridge Structure

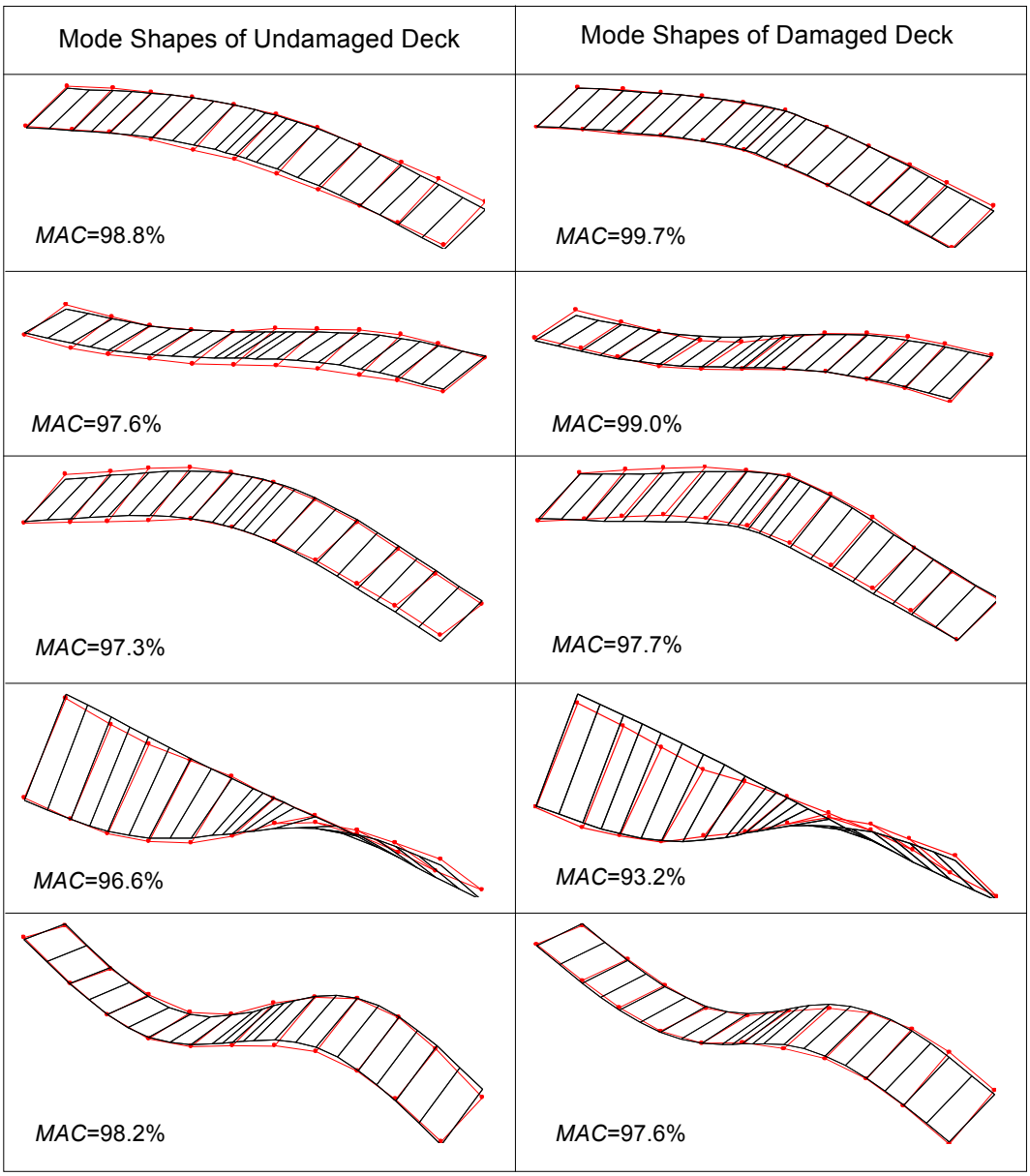

Fig. 13 Pair of Mode Shapes between FE Updated and Measured
——FE Updated —●— Measured

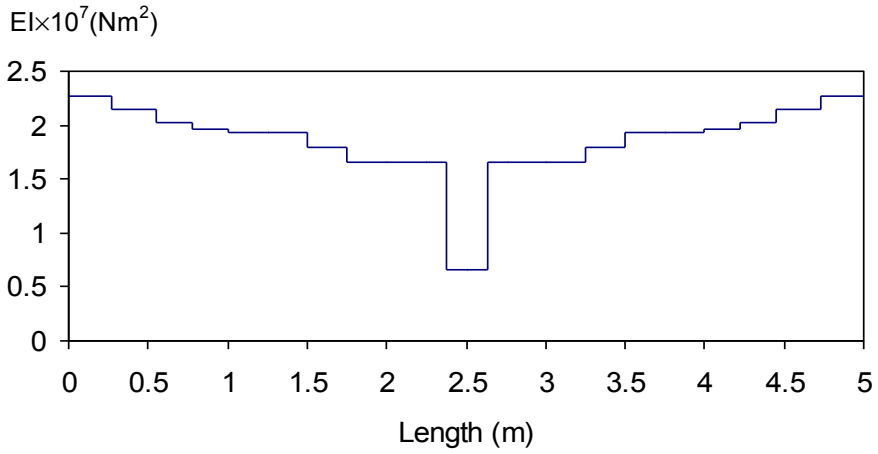

Fig. 14 Distribution of Stiffness of Failed Beam

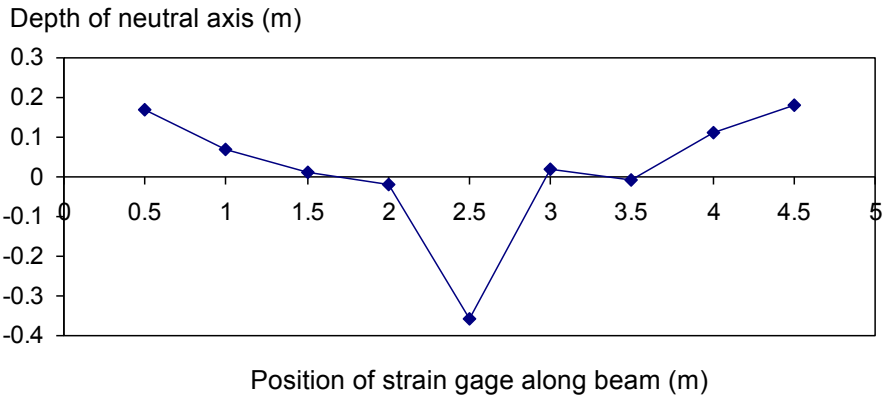

Fig. 15 Measured Neutral Axis of Beam under Ultimate Limit State

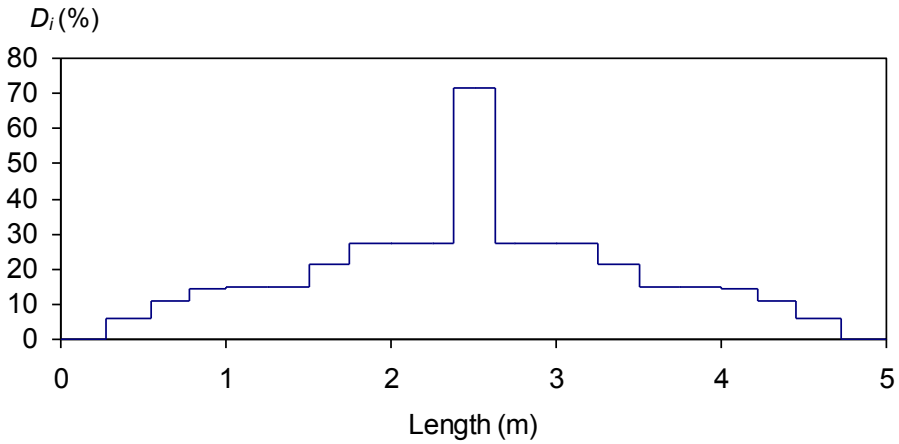

Fig. 16 Distribution of Damage Index along Beam